Journal of Chromatography A, 1218 (2011) 4188–4198

Contents lists available at ScienceDirect

Journal of Chromatography A

journal homepage: www.elsevier.com/locate/chroma

Characterization of aquatic dissolved organic matter by asymmetrical flow field-flow fractionation coupled to UV–Visible diode array and excitation emission matrix fluorescence

Céline Guéguen*, Chad W. Cuss

Chemistry Department, Trent University, 1600 West Bank Drive, Peterborough, Ontario K9J7B8, Canada

ARTICLE INFO

Article history:
Available online 24 December 2010

Keywords:
Dissolved organic matter
Optical properties
Excitation emission matrix
UV/Visible absorbance
Athabasca River
Humic

ABSTRACT

Flow field-flow fractionation (FlFFF) with on-line UV/Visible diode array detector (DAD) and excitation emission matrix (EEM) fluorescence detector has been developed for the characterization of optical properties of aquatic dissolved organic matter (DOM) collected in the Otonabee River (Ontario, Canada) and Athabasca River (Alberta, Canada). The molecular weight (MW) distribution of DOM was estimated using a series of organic macromolecules ranging from 479 to 66,000 Da. Both the number-average (M_n) and weight-average (M_w) molecular weights of Suwannee River fulvic acid (SRFA) and Suwannee River humic acid (SRHA) determined using these macromolecular standards were comparable to those obtained using polystyrenesulfonate (PSS) standards, suggesting that organic macromolecules can be used to estimate MW of natural organic colloids. The MW of eight river DOM samples determined by this method was found to have an M_n range of 0.8–1.1 kDa, which agrees with available literature estimates. The FlFFF-DAD-EEM system provided insight into the MW components of river DOM including the optical properties by on-line absorbance and fluorescence measurement. A red-shift in emission and excitation wavelength maxima associated with lower spectral slope ratios ($S_R = S_{275–295}:S_{350–400}$) was related to higher MW DOM. However, DOM of different origins at similar MW also showed significant difference in optical properties. A difference of 47 and 40 nm in excitation and emission peak C maxima was found. This supports the hypothesis that river DOM is not uniform in size and optical composition.

1. Introduction

The colored or chromophoric fraction of the DOM pool (CDOM) which absorbs light in the UV/Visible spectral region, has been extensively studied in both fresh and marine waters [1–4]. CDOM is thought to play a key role in limiting light penetration, the regulation of microbial activity, and in pollutant and heavy metal binding, transport, and bioavailability [5–9].

The main sources of DOM in natural waters are terrestrial inputs and in situ production by plankton, which contribute to changes in its structural and optical characteristics [10]. For example, CDOM of terrestrial origin displays excitation and emission maxima at longer wavelengths than do marine materials, as a result of their more aromatic chemical nature and higher molecular weight [11]. The majority of DOM released by phytoplankton in the oceans consists of low molecular weight organic molecules (~30–50% of dissolved organic carbon (DOC); [12]). In contrast, terrestrial river-borne DOM is dominated by colloidal macromolecules (up to 86% of DOC; [13]). Little is known about the optical properties of colloidal DOM, however, even though the colloidal fraction is predominant in the freshwater DOM pool.

Size distributions of DOM can be determined experimentally by ultrafiltration [12–14]. Ultrafiltration enables large quantities of size-fractionated DOM to be isolated for structural, elemental and isotopic analysis. However, only discrete fractions of materials can be isolated using this method. Recently, flow field-flow fractionation (FlFFF) has been applied to DOM to obtain continuous molecular size information [15–17]. Flow FFF is a chromatography-like analytical separation technique for the fractionation of macromolecules from 0.001 to >1 μm [18]. One of the major advantages of FlFFF is the ability to obtain a continuous size distribution of macromolecules that may be analyzed further by coupling additional detection instruments on-line, or by using off-line detectors after collecting volume fractions [19]. By coupling on-line detectors, more detailed information can be obtained. For example, fine-scale variations observed in the optical properties of the samples can then be investigated in relation to the MW distribution.

Absorbance detection (UV–VIS) at fixed wavelengths (e.g. 254 nm) constitutes the detector of choice in FlFFF studies, as it is

* Corresponding author. Tel.: +1 705 748 1011.
E-mail address: celinegueguen@trentu.ca (C. Guéguen).

0021-9673/$ – see front matter © 2010 Elsevier B.V. All rights reserved.
doi:10.1016/j.chroma.2010.12.038

Table 1
Physical chemical characteristics of river DOM analyzed in this study.

Station ID	pH	Conductivity [μS/cm]	DOC [ppm-C]
Otonabee R.			
OR01	7.40	235	9.3
Athabasca R.			
AR01	8.02	242	5.6
AR02	8.14	244	7.0
AR03	8.07	189	15.9
AR04	7.77	225	15.8
AR05	7.73	237	12.2
AR06	8.02	240	20.0
AR07	7.95	233	14.5

used to generate the MW calibration curve [17,20,21]. Recently, the UV/Visible diode-array detector (DAD) has been coupled to FlFFF to obtain the entire UV/Visible spectra of eluting samples instead of monitoring only a fixed wavelength [15,22]. This allows for the determination of *S*-parameter as a function of DOM size.

Unlike absorbance, very few studies have coupled fluorescence detectors to FlFFF [15,23,16,24]. Moon et al. [24] found no significant variation in the mean size of DOM using protein fluorescence detection, whereas Zanardi-Larnardo et al. [15] and Hassellöv [16] found significant variation in MW distribution using humic-like fluorophores. This illustrates that the study of MW distribution of DOM fluorophores should be monitored at various wavelengths, allowing for the detection of variation in multiple fluorophores. Recently, excitation emission matrix (EEM) fluorescence analyses of discrete fractions from the FlFFF channel outflow collected at different elution times showed that the fluorescence signature changed with molecular sizes [25]. Although based on limited number of samples, Boehme and Wells [25] showed that fluorophore characteristics are size-dependent.

The current work presents the first reported coupling of an asymmetrical FlFFF separation chamber to online UV/Vis diode array and excitation emission matrix fluorescence detectors (AsFlFFF-DAD-EEM) for the purpose of analyzing the fine scale distribution of size-based optical properties of aquatic DOM.

2. Materials and methods

2.1. Standards and samples

All glassware used for the preparation of standards, sampling and storage was pre-washed with Milli-Q water and combusted at 450 °C for 5 h prior to use. Teflon-lined caps were acid washed in 10% nitric acid, rinsed in Milli-Q water, and allowed to air dry for 24 h before being used.

Suwannee River fulvic acid (SRFA, 2S101F) and Suwannee River humic acid (SRHA, 2S101H), obtained from the International Humic Substances Society were used without further purification, but were dissolved in carrier solution at concentrations in the range of 5–10 mg carbon L^{-1} (ppm-C).

The freshwater samples were collected in summer 2009 from the Athabasca (AR) and Otonabee (OR) rivers (Table 1). The samples were immediately filtered on site through a pre-combusted GFF filter and stored at 4 °C in pre-combusted amber glass vials until analysis. DOC content was measured on a Shimadzu TOC-V_{CPH}. The samples were also diluted to 5–10 ppm DOC with carrier solution prior to AsFlFFF injection if DOC concentration was higher than 10 ppm-C.

2.2. Instrumentation and setup

AsFlFFF fractionation was carried out using an AF2000 Focus fractionation system (Postnova Analytics, Landsberg, Germany) which included two PN1130 HPLC pumps to control the axial and focus flows, a PN1610 syringe pump to control the crossflow rate, and a PN7505 degasser to remove gas from the carrier solution prior to introduction to the pumps.

Reagent grade sodium chloride (58 ppm, ~220 μS/cm; Caledon Laboratories Ltd.) was used to adjust the ionic strength of the Milli-Q water to within the range of natural waters. This solution formed the carrier solution for the AsFlFFF experiment.

0.1 μm in-line PVDF filters (Millipore) were placed in the carrier lines before entering the channel in order to retain any particulate impurities that might come from the pumps.

The fractionation system was equipped with a 300Da polyethersulfone (PES, Postnova Analytics) membrane and a 500 μm spacer. Flow settings for the separation procedure were set to 0.3, 3.3, and 3.5 mL/min axial, focus, and cross flows, respectively, during the focusing stage, and this cross flow volume was maintained during elution. Flow rates were optimized based on a compromise between peak resolution using the calibration standard mixture and a reasonable separation time. Membrane-specific channel dimensions were not determined, as they are not required using the macromolecular calibration method. The separation was carried out with a channel length and area of 27.5 cm and 3160 mm^2, respectively. The void and dead volumes were ~1122 mL and 1 mL, respectively. The AsFlFFF system is equipped with pressure sensors preventing system overpressure. System pressure was not an issue during the experiment, despite the high crossflow rate and small membrane pore size.

Approximately 2 mL of each sample was injected into the Rheodyne injection valve with a 0.9 mL sample loop in order to condition the loop and minimize memory effects, and its overflow passed into a waste container.

Absorbance scans were recorded from 250 to 700 nm every 0.640 s using an on-line Shimadzu SPD-M20A UV/Vis diode array detector (DAD). Absorption coefficients a_λ (m^{-1}) at each wavelength λ were calculated as follows:

$$a_\lambda = \frac{2.303A(\lambda)}{l}$$

where $A(\lambda)$ is the absorbance at wavelength (λ) and l is the optical path length in meters. The spectral slope of the absorption spectrum S was calculated using a non-linear fit [1] in SigmaPlot 10 (Systat Software Inc.) [26]. The slope parameters ($S_{275–295}$ and $S_{350–400}$) were computed from 275 to 295 nm and 350 to 400 nm, respectively [27].

On-line fluorescence signals were monitored at 270/460 and 355/460 nm using an Agilent 1200 series fluorescence detector (Model G1321A). The excitation/emission pairs were chosen based on the fluorescence maxima of bulk samples. On-line EEM scans were recorded at excitation wavelengths from 220 to 515 nm and emission 280 to 700 nm in increments of 1 nm for excitation and 5 nm for emission. The Raman peak intensity at excitation 350 nm was used to standardize fluorescence intensity.

M_p is defined as the MW corresponding to the peak maximum. The number-average (M_n) and weight-average (M_w) molecular weights were determined using the following equations [28]:

$$M_n = \frac{\sum_{i=1}^{n} h_i}{\sum_{i=1}^{n} \frac{h_i}{M_i}}$$

$$M_w = \frac{\sum_{i=1}^{n} h_i M_i}{\sum_{i=1}^{n} h_i}$$

where h_i is the detector response of the sample FlFFF curve eluted at retention time $(R_t)i$ and M_i is the molecular weight at retention time i, as determined from the standard calibration curve.

2.3. Calibration

To obtain a realistic MW calibration, the standards must resemble the analyte colloids in their density, shape, and relevant physical properties. This could be challenging because of the heterogeneous nature of DOM [29]. Polystyrene sulfonate (PSS) standards have been used for DOM analysis by FlFFF in the past [20,30]. Unfortunately, PSS standards generally have MW values above those of humic substances which are the primary components of DOM, so that measurement of DOM using these standards requires the statistically questionable extrapolation of the regression line. However, proteins with similar optical and electrochemical properties to DOM have recently been used to estimate the MW distribution of aquatic colloids by FlFFF-UV-ICPMS [31].

Calibration was performed with macromolecules: laser grade rhodamine B (479 Da; Acros Organics), Trypan blue (961 Da; Sigma–Aldrich), vitamin B12 (1330 Da; Sigma–Aldrich), bovine heart cytochrome C (12,400 Da; Sigma–Aldrich), hen egg white lysozyme (14,000 Da; Fluka) and bovine serum albumin (66,000 Da; Sigma–Aldrich), were prepared in the carrier solution. A log–log retention time versus MW calibration curve was plotted and subsequently used to calculate the MW of samples. The large macromolecule bovine serum albumin (66,000 Da) was used to ensure that any larger DOM molecules would be included in the linear range. However, neither the slope nor the correlation coefficient changed significantly when the higher MW standard was removed from the calibration regression.

Percent mass recoveries of DOM were estimated at 35% by comparing the absorbance peak areas of non-fractionated Suwannee River fulvic acid (5 ppm; 2S101F, IHSS) to those of fractionated samples at 254 nm, which is within the range reported in the literature [15,30]. Carrier solution was injected before all samples and standards to ensure the absence of memory effects and the membrane, separation chamber, and sample path were flushed and cleaned with carrier solution as necessary between samples. Calibration standards were injected both as singular solutions and in mixtures to be certain that the retention times of the multi-constituent fractograms corresponded to particular molecules, and hence to the molecular weight thereof. The retention times of the peak maxima were normalized to the appearance of the void peak obtained with the DAD and EEM detectors.

2.4. Statistical analysis

Principal component analysis (PCA) is a statistical technique used to group interrelated variables into linearly independent linear combinations, or components, which explain the variance between samples as measured over a range of parameters. Since the first few components often account for the majority of this multidimensional variation, PCA effectively reduces the dimensionality of the data set enabling the differentiation of samples that may otherwise prove difficult to distinguish [32].

Given the large amount of data provided by fluorescence EEMs and the significant number of other measurements available for testing the molecular weight and size-based characteristics of DOM, statistical techniques like PCA are frequently employed to reduce the dimensionality of data sets to a more manageable level [33–36]. Other common statistical techniques such as PARAFAC and PLS analysis require data sets that are larger than those available for the purposes of this study [26,36]. Hence, PCA was employed to gauge the relative usefulness of the fractionation procedure in the separation of the molecular weight fractions by assessing patterns of variation in size-based indicators, both within and between samples. The PCA was carried out using the MW from AsFlFFF-DAD-EEM, a_{254}, a_{355}, S_R, $S_{275–295}$, the ratio of absorption coefficients at 250 nm to that of 365 nm (E2/E3) [37], and the maximum fluorescence intensities for humic-like peaks (peaks A and C, Ex/Em 237–260/400–500 nm and 300–370/400–500 nm, respectively [4]). PCA was completed using version 2.11.0 of the statistical software R, distributed under the terms of the GNU General Public License.

Table 2
M_n, M_w and M_p obtained in SRFA, SRHA and river samples.

Station ID	M_n	M_w	M_p	M_w/M_n
SRFA	1262	2155	1089	1.71
SRHA	1605	5692	2305	3.55
Otonabee R.				
OR01	795	989	870	1.24
Athabasca R.				
AR01	848	1099	938	1.30
AR02	844	1093	859	1.29
AR03	948	1369	1011	1.44
AR04	1114	1557	1276	1.40
AR05	941	1210	1276	1.29
AR06	902	1207	974	1.34
AR07	1000	1372	1089	1.37

3. Results and discussion

3.1. Molecular weight calibration

The estimated molecular weight distributions were obtained by calibrating the AsFlFFF system with a series of organic macromolecules with molecular weight ranging from 479 to 66,000 Da. These macromolecules have been useful for calibrating ultrafiltration membranes in other studies of the MW of aquatic colloidal DOM [13,38].

In order to check the validity of our macromolecule-based MW calibration, the MW determined for Suwannee River fulvic and humic acid (SRFA and SRHA) standards were compared to the MW distribution previously determined by FlFFF and other methods. For SRFA, the calculated M_n, M_w and polydispersity (M_w/M_n) were 1262, 2155 and 1.71 Da (Table 2). This agrees with previously reported values (M_n = 1105–1658, M_w = 1910–2364 and M_w/M_n = 1.43–1.76 Da [20,38–40]). Similarly, the M_n and M_w of SRHA determined by FlFFF using PSS calibration lie in a range of 1500–2400 Da and 2400–4400 Da [20,40–42], respectively, which also agrees quite well with the values determined in this work. This establishes that calibration using organic macromolecules can be used to estimate MW of organic colloids.

Calibrations at 254 nm and 270 nm were typically established in DOM studies [20,16,25,43], but there is no general consensus on using any particular wavelength to estimate the MW distribution using UV detection. The diode array detector (DAD) allowed investigation of the potential impact of the operating wavelength on the MW determination. Calibration curves at wavelengths ranging from 254 to 275 nm were plotted and the impact on MW distribution investigated (Table 3). The identical correlation coefficients highlight the consistency of results across absorption wavelengths. The M_n of natural DOM samples ranged from 826 to 844 Da depending on the absorbance wavelength used. The variability in M_n, M_w and M_p were less than 1% on average between wavelengths, and thus calibrations at wavelength from 254 to 275 nm were considered to be similar. Since greater absorbance values are generally observed at lower wavelengths, this evidence suggests that shorter absorbance wavelengths (e.g. 254 nm) are preferable for monitoring the MW distribution. Although wavelengths shorter than 254 nm can detect even more chromophores, measurement at these wavelengths is not recommended as some inorganic species such as nitrate may interfere [44], and the concentration of small particles may also be underestimated [45].

The MW distribution of macromolecule mixtures was compared to single macromolecule solutions single macromolecule solutions

Table 3
M_n, M_w, M_p of natural DOM measured at 254, 260, 265, 270 and 275 nm using UV detection.

UV detection	M_n	M_w	M_p	Calibration curve[a]
254 nm	844	1093	859	log rt = 0.132 log MW + 0.416, r^2 = 0.943
260 nm	832	1067	843	log rt = 0.135 log MW + 0.408, r^2 = 0.943
265 nm	834	1070	844	log rt = 0.135 log MW + 0.408, r^2 = 0.943
270 nm	826	1068	836	log rt = 0.134 log MW + 0.412, r^2 = 0.942
275 nm	839	1077	847	log rt = 0.135 log MW + 0.408, r^2 = 0.942

[a] Calibration curves (equation and r^2) were determined using macromolecules (see text for more details).

(Figs. 1 and 4). It can be noted that absorbance of rhodamine B is greater near 550 nm than at 254 nm (Fig. 4). The retention time of each macromolecule in the mixture was similar to those in single solutions (difference less than 0.07 min). No significant difference in M_p was found between single and mixture standards. Thus, the FlFFF system is capable of separating and detecting organic macromolecules of similar MW using the developed procedure.

3.2. Linear range and reproducibility

In order to check the linearity of response of the FlFFF system, different concentrations of vitamin B12 (5–30 ppm; Fig. 2A) and DOM (2–10 ppm-C; Fig. 2B) were injected and the MW distribution was estimated. The range of concentrations used here (2–10 ppm-C) was consistent with DOM concentration typically found in natural rivers. The linear response (R^2 = 0.99 at 254 nm) demonstrated that high concentrations of macromolecules and DOM can be used without compromising the integrity of the FlFFF membrane. The retention times at peak maximum were within 6 s, corresponding to 165 Da, which is considered to be negligible (see below discussion on reproducibility). It is also notable that the peak shape of each remained unchanged regardless of their natures and concentrations.

Though the MW distribution in DOM-rich samples can be estimated, limiting cross contaminations requires extensive cleaning and time-consuming cleaning steps, which could significantly reduce sample throughput. Further, high DOC concentration (>10–15 ppm-C) increases the effects of inner filtering in fluorescence [46]. In this work, low to moderate DOC samples (5–10 ppm-C) were injected directly, whereas DOC-rich samples (>10 ppm-C) were diluted to this concentration range with carrier solution prior to analysis.

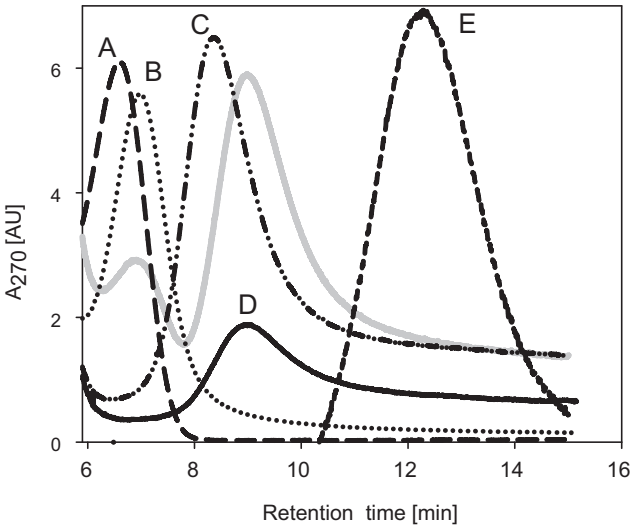

Fig. 1. Fractograms of mixture (vitamin B12+ cytochrome C; gray) and single standards (A – Trypan blue, B – vitamin B12, C – lysozyme, D – cytochrome C, E – bovine serum albumin).

The standards were analyzed routinely to ensure continual system integrity over the course of the analysis. A day-to-day difference of only 1.1% RSD, 0.0004 nm^{-1} and 0.15 AU was reported for MW averages of standards, spectral slopes and fluorescence intensities, respectively (n = 7). This demonstrates that the FlFFF-based MW is sufficiently precise to note differences of ~100 Da. Our results showed that an accurate and comparable MW estimate of DOM can be obtained by FlFFF.

3.3. MW distribution of river DOM

Typical fractograms of DOM samples are shown in Fig. 3. Resulting values for the number averaged, weight averaged, and peak molecular weights, as well as the polydispersity are included in Table 2. Values for M_n and M_w ranged from 795 to 1114 Da and from 1093 to 1557 Da, respectively. Based on the limited number of existing studies, M_n of river DOM determined by FlFFF using PSS calibration and UV detection lie in a range of 670–2113 Da [15,41,43,47,48], which are quite similar to the values determined in this work.

Absorbance and fluorescence detectors were sequentially online during the FlFFF experiment allowing for direct comparison of the results. The MW distribution for fluorescence was shifted towards slightly lower MW relative to that obtained for absorbance (Fig. 3). Chromophores and fluorophores in the AR samples were centered at 1030 ± 160 (n = 7, 1σ) and 850 ± 120 Da (n = 7, 1σ), respectively. This suggests that chromophores did not have the same MW distribution as the fluorophores. Also, some of the absorbing moieties either did not fluoresce or fluoresced less intensively than their lower MW counterparts. Similar results were found in studies of DOM in rivers and coastal waters [15]. Although based on only a single sample, the OR sample showed a significantly lower M_p than in the AR system. The AR passes through a wetland region, resulting in a higher MW distribution. On the other hand, the OR arises from a series of lakes and reservoirs that form the Trent-Severn Waterway where large molecules have likely settled, which is consistent with a lower MW distribution.

Conducting field research often involves storing samples, which is typically performed in the dark at 4 °C. To test the effect of storage on DOM MW determination, the MW distribution of a river sample (i.e. OR01) was determined over a period of 7 days from the sampling day. M_p ranged from 825 to 901 Da with an average of 854 ± 33 Da (n = 10, 1σ). The 4% variation is lower than that found over the M_p of natural samples measured in this study (417 Da; Table 2), suggesting that a 7-day storage does not significantly affect MW distribution.

3.4. Optical properties and molecular size distribution

A typical output from the AsFlFFF-DAD-EEM is displayed in Fig. 4. The combination of diode array and EEM detectors allows a more comprehensive picture of the optical properties of DOM along with its MW distribution. This is particularly pertinent as it allows the linkage of optical features to DOM size.

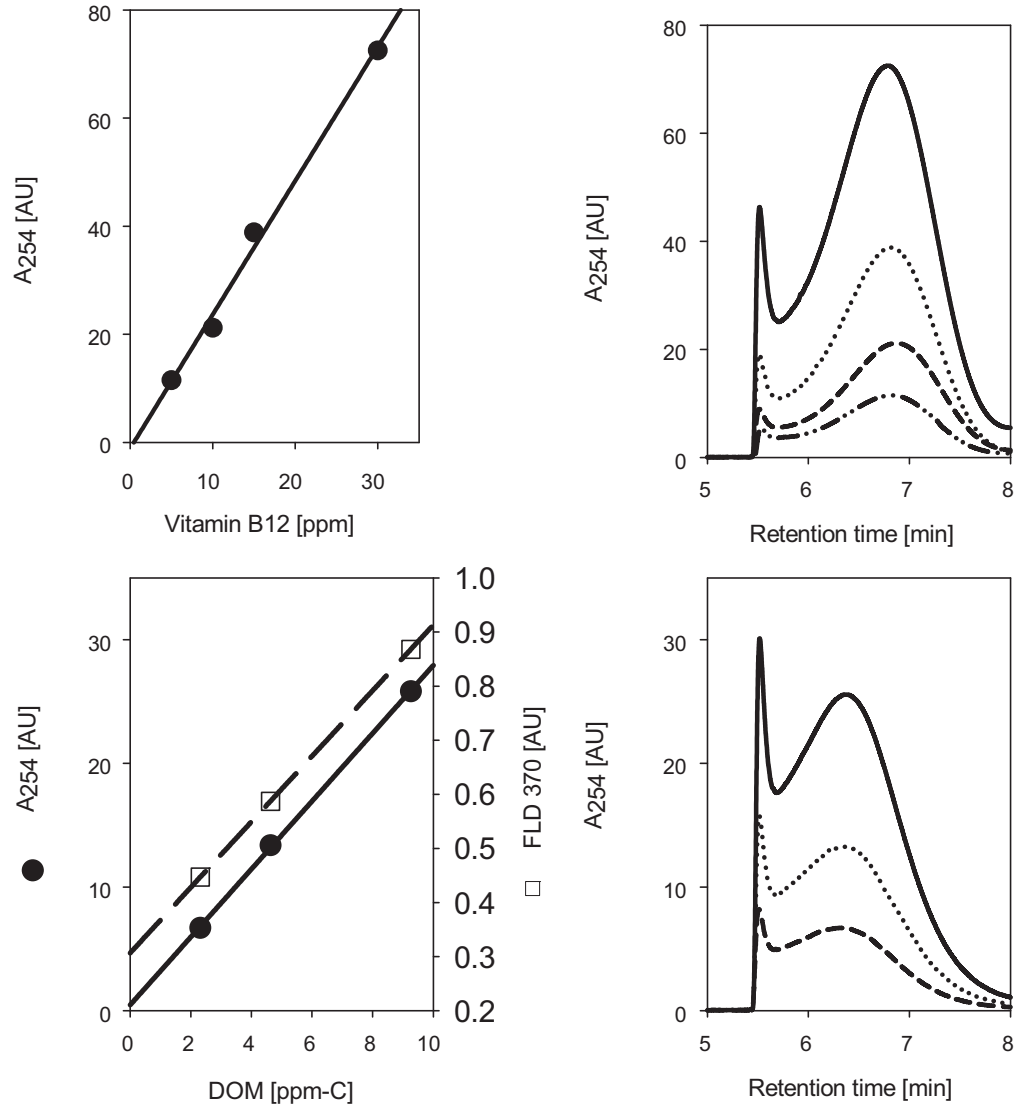

Fig. 2. Linear response and peak area for vitamin B12 (1.33 kDa; upper panels) and OR01 (bottom panels). The determination coefficients of least square linear regression equations are >0.99 for both detectors (DAD, line; FLD; dashed) and analytes.

The on-line absorbance detector coupled with the continuum size separation offered by AsFlFFF was used to assess variations in spectral slopes (S) as a function of MW. Spectral slope offers further insights into the characteristics (e.g. source and nature) of DOM than absorption alone. The spectral slope of the DOM samples varied greatly with retention time and thus MW (Fig. 5). For example, the spectral slope ratio ($S_R = S_{275–295}/S_{350–400}$ [26]) decreased from 1.00 to 0.84 as MW increased from ~300 to 2500 Da

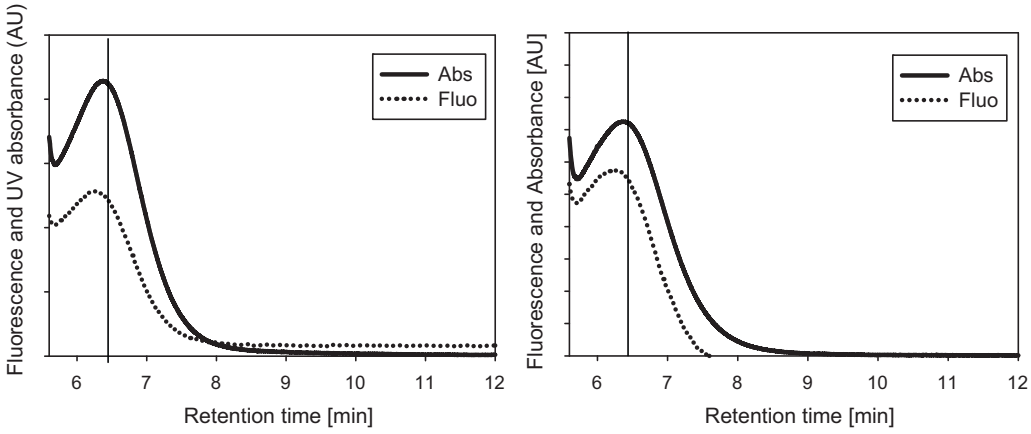

Fig. 3. Fractograms of fluorescence and absorbance from two DOM samples (OR01 left; AR02 right).

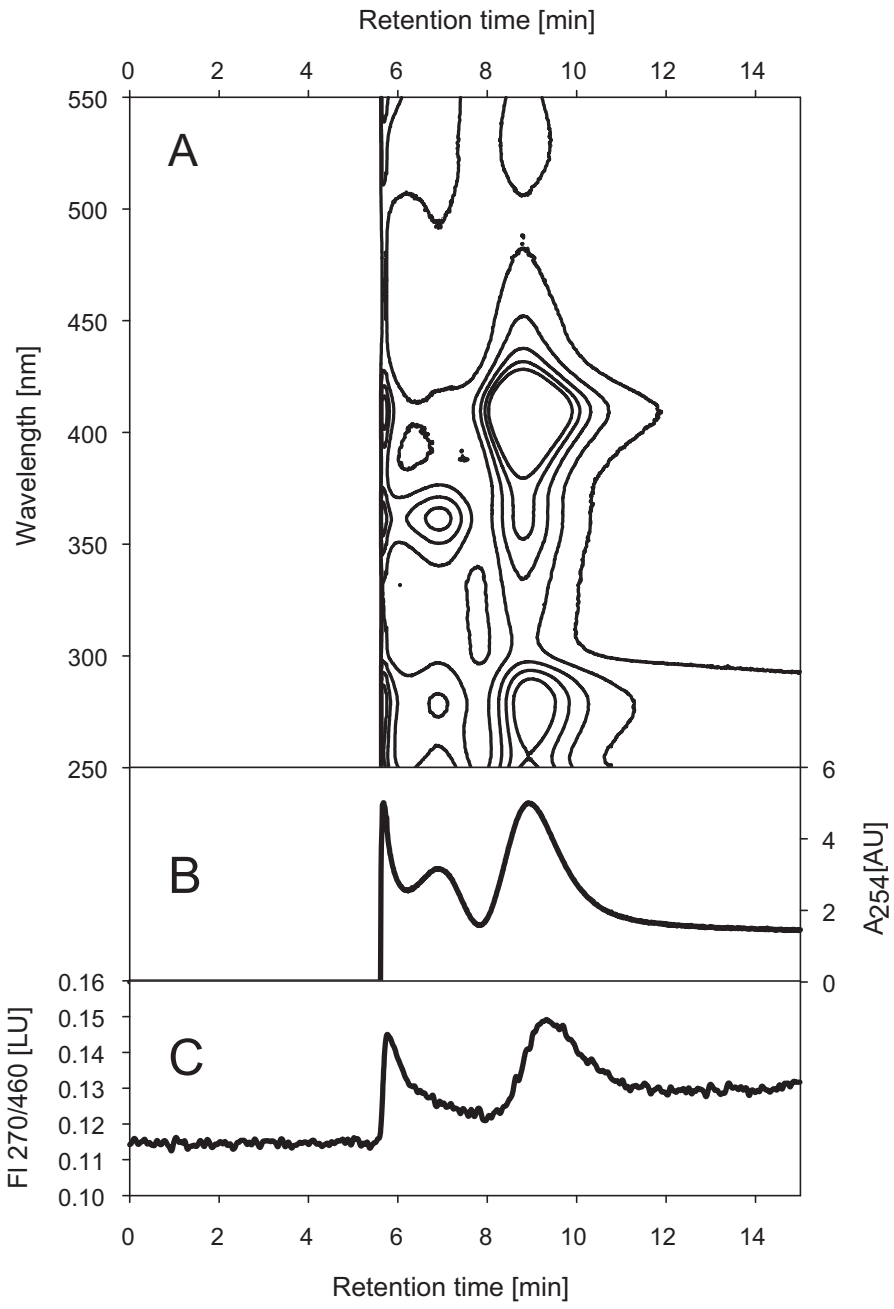

Fig. 4. Fractogram profiles showing (A) the absorbance scan (250–550 nm), (B) the absorbance at 254 nm, (C) the fluorescence detection (Ex 270/Em 460) of macromolecule mixture (10 ppm rhodamine B + vitamin B-12 + cytochrome C) obtained by AsFlFFF-DAD-EEM.

in OR01 (Fig. 6). This suggests that the increase in MW, as measured herein using AsFlFFF, shifts the absorption spectrum towards longer wavelengths [37,49] causing steeper $S_{350–400}$ and decreased S_R.

The AsFlFFF data presented in this study suggest that spectral shifts in S_R are linearly correlated with changes in MW (Fig. 6; Table 4). A similar trend was observed for aquatic DOM using SEC [26]. The observed ranges in the S_R parameter were 0.76–1.06 in this study, which are similar in range to those reported for the CDOM-rich waters from the Great Dismal Swamp (0.68–1.11; [26]) and Venezuelan tropical rivers (0.61–1.06; [50]). Although strong negative correlation between S_R and MW was found in all DOM samples analyzed in this study, the relationship was variable among samples (Table 4). This agrees well with the natural variability in chromophoric composition, and thus spectral slopes of DOM [22]. The spectral slopes $S_{275–295}$ and $S_{350–400}$ appear to be linearly related to MW, but only at MW higher than 600–800 Da (Fig. 5). This suggests that $S_{275–295}$ and $S_{350–400}$ can be indicative of shifts in high MW range (1000–2500 Da), but cannot be used as reliable proxy for low MW (<800 Da). These results are consistent with the trend of

Table 4
Parameters of linear regression S_r = slope × MW + intercept ($p < 0.001$).

	Slope	Intercept	r^2
OR01	−7.97E−05	1.036	0.986
AR01	−1.06E−04	1.074	0.894
AR02	−9.23E−05	1.092	0.889
AR03	−7.73E−05	0.909	0.962
AR04	−5.95E−05	0.927	0.973
AR05	−1.01E−04	1.001	0.958
AR06	−8.10E−05	0.935	0.983
AR07	−8.98E−05	1.000	0.975

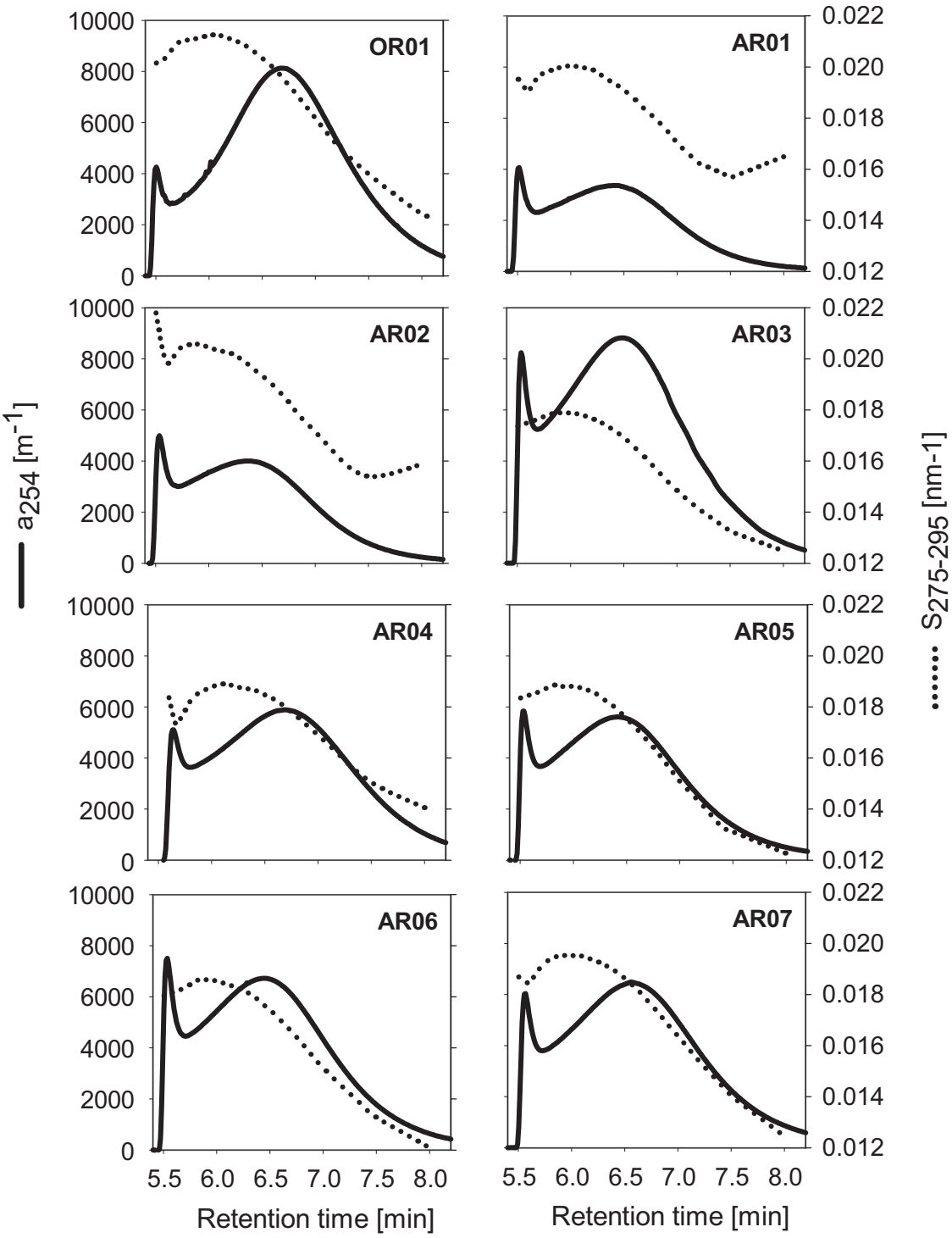

Fig. 5. Fractograms obtained by Fl-FFF-DAD-EEM of river DOM.

decreasing relation between $S_{275-295}$ and $S_{350-400}$ with MW ranging from 1000 to 3000 Da, as determined by SEC [26].

The range of spectral slopes observed at peak maximum (S_{M_p}) for the interval 275–295 nm was 0.0170–0.0198 nm^{-1} in river samples, which is typical of river samples [26,27]. Higher spectral slopes were not found at M_p, but are associated with lower MW compounds (Fig. 5), which may result from size-related chromophoric differences.

EEM analyses showed that the DOM fluorescence characteristics varied across a range of MW. The EEM results for four retention times for the Athabasca River sample (AR05) are shown in Fig. 7; the small-sized fraction ($R_t < R_{tM_p}$; a-fraction; Fig. 7a), at peak maximum ($R_t = R_{tM_p}$; b-fraction; Fig. 7b) and the large-sized fractions ($R_t > R_{tM_p}$ and $R_t \gg R_{tM_p}$; c- and d-fractions; Fig. 7c and d). The lines mark the position of the peak C in a-fraction. The contour plots at four R_t show the dominance of two pairs of peak maxima corresponding to a humic-like signature, identified here using the labeling convention of peaks A and C [51]. The peak A wavelength maxima (Ex_{max}/Em_{max}) occurred at 237–241/420–445 nm. The peak C fluorescence excitation and emission maxima ranged from 300 to 347 nm and from 420 to 460 nm, respectively. Protein-like fluorescence (Ex 225–280/Em 300–340; [51]) was detected

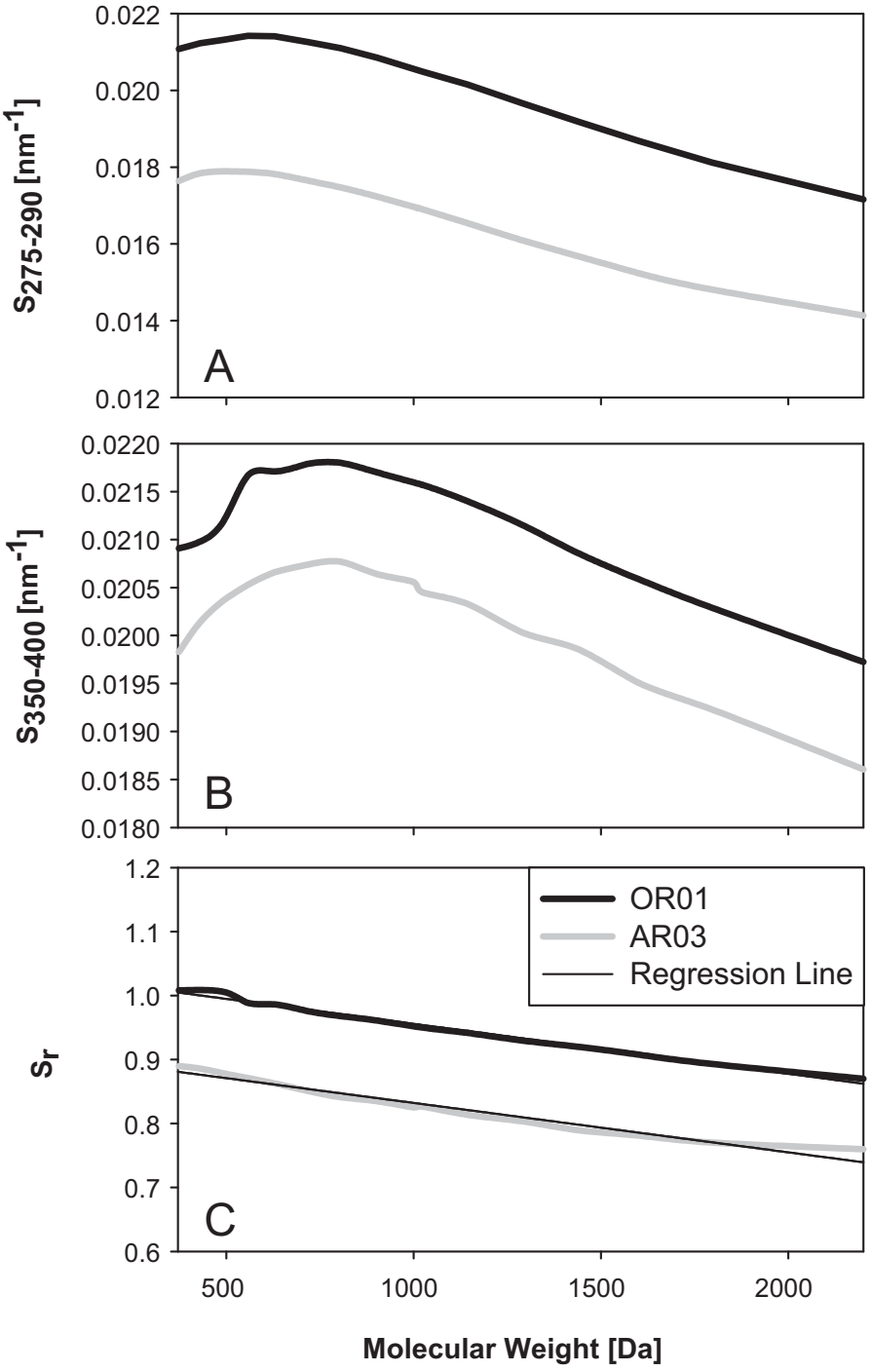

Fig. 6. (A and B) Slope parameters versus molecular weight and (C) ratio of spectral slope versus molecular weight of DOM as determined by AsFlFFF-DAD-EEM.

at low intensity (<0.1 r.u.) at $R_t < R_{tM_p}$ and $R_t = R_{tM_p}$, but not in the large-sized fractions. This contrasts with the study of estuarine DOM during a plankton bloom where protein-like fluorescence was dominant in the small-sized fractions [25]. Protein-like fluorophores have been considered labile components [52], produced by biological activity in the water column [53,54]. Their low fluorescence intensity indicates that the production of algal-derived DOM may comprise a minor fraction of the river DOM detected by the AsFlFFF-DAD-EEM system.

The EEM data suggests that there are significant differences in the fluorescence characteristics of different DOM size fractions. The fluorescence intensity maxima of peak C were shifted to longer excitation and emission wavelengths with increasing MW (i.e. increasing R_t) (Figs. 7 and 8). For example, the position of the excitation fluorescence maxima in AR06 varied from 326 to 347 nm in a- and d-fractions, respectively, while the emission maxima varied from 425 to 460 nm. Those changes in peak position were significant given wavelength increments of 1 and 5 nm on excitation and emission, respectively. A similar red shift in fluorescence has been noted in ultrafiltration studies, suggesting that high MW DOM is characterized by a higher wavelength maximum relative to low MW compounds [3,13,55]. This red shift in the peak has also been attributed to increasing hydrophobicity, aromaticity [56] and oxidized forms [57] in higher MW constituents. This result

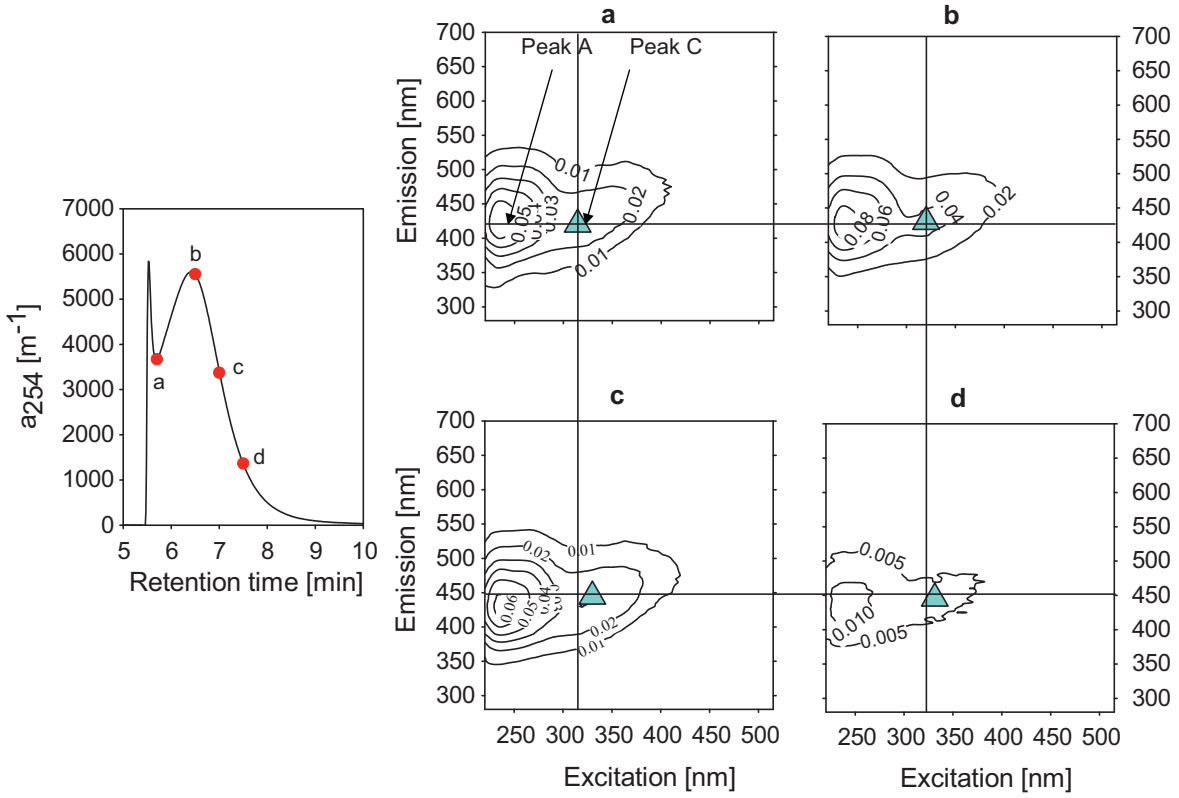

Fig. 7. A fractogram profile showing the retention time (R_t) of the four EEMs (a) the small-sized fraction ($R_t < R_{tM_p}$), (b) at peak maximum ($R_t = R_{tM_p}$) and (c and d) the large-sized fractions ($R_t > R_{tM_p}$ and $R_t \gg R_{tM_p}$). Peak C maxima (blue triangle) are indicated for each fractions. Lines indicate Peak C maxima in a-fraction. (For interpretation of the references to color in this figure legend, the reader is referred to the web version of the article.)

is congruent with the increase in spectral slope observed with decreasing MW [Fig. 5]. Although the humic-like signature was predominant in the river DOM isolated by FlFFF-DAD-EEM, the fluorophoric composition varied among samples at any given MW. For example, the peak C wavelength maxima (Ex_{max}/Em_{max}) at ~1250 Da ranged from 318/430 nm to 331/445 nm at AR02 and AR06, respectively (Fig. 8). This indicates that the composition of DOM at R_{tM_p} was not the same for these river samples. No relationship between peak C characteristics and MW at R_{tM_p} were found, illustrating that the fluorescence characteristics were not found to be size-dependent. The variability in fluorescence peak maxima associated with size-dependent differences in chromophoric composition clearly implies that the optical composition of DOM is non-homogeneous.

3.5. Principal component analysis (PCA)

The statistical analysis of the size-based optical properties of DOM as determined using AsFlFFF revealed distinct differences among MW fractions and samples. The first and second principal components for the AR samples accounted for 59 and 36%, respectively, of the total variance. MW had strong positive weightings on both PCA axes (Fig. 9A). The MW proxies (i.e. E2/E3 ratio and spectral slope parameters $S_{275–295}$ and S_R) as derived from absorbance analysis had negative weightings on both PCA axes. The MW proxies and FlFFF-based MW were found to have diametrically-opposing PCA loadings. Since it is known that the MW proxies are negatively correlated with MW, this reinforces the significance of MW determination using AsFlFFF.

Plotting the AR sample scores for PC1 and PC2 on separate axes (Fig. 9B) revealed clustering of the samples by MW fraction, with the greatest weight fraction (i.e. d-fractions) well-separated from the others. The PC1 could discriminate samples mainly according to the MW. The small weight fractions of each sample (i.e. a and b fractions) were grouped at the left side of the graph and the larger fractions (c and d fractions) towards the right. The smallest-sized fractions (a-fraction) were clustered together with negative weightings on both axes (except AR03) whereas the b-fractions were evenly distributed along PC2. Taken together, this result indicates that the size fractions showed important variability in optical properties with the largest fractions having the greatest difference.

The PCA also revealed differences between samples. Two of the samples (AR01 and AR02) were clustered together in the bottom section of the graph (negative PC2). These two samples were taken ~500 km upstream from the AR03-07 sites which were located near a major industrial project along the banks of the Athabasca River, suggesting that some alteration of the DOM may have taken place. On the other hand, the downstream samples AR03-07 contributed positively to PC2 with the exception of their smallest size fractions which had a slightly negative effect in this axis. This indicates that these downstream samples had similar MW and optical properties. Taken together these results reveal significant variability in the optical properties of DOM isolated by AsFlFFF. More importantly, they indicate that the developed AsFlFFF method may be useful in the detection of source-based differences in DOM.

The limited number of samples and small geographic area analyzed in this study make it difficult to draw confident conclusions about size-based differences in DOM. However, the fact that samples of only moderately disparate origins have been distinguished using relatively few samples suggests that this procedure may be a useful ingredient in both the characterization and size-based source differentiation of DOM.

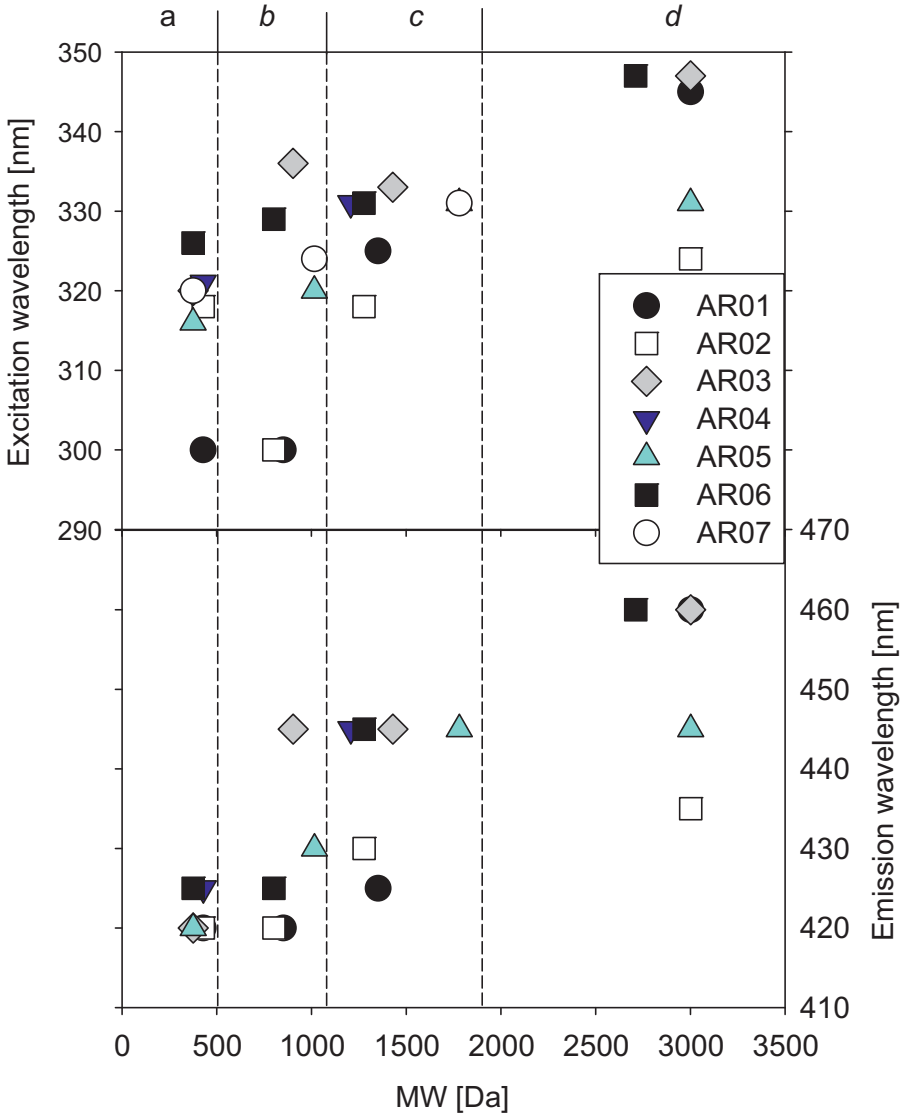

Fig. 8. Position of the excitation and emission peak C maxima at four retention times for the Athabasca River sample (AR05). a-, b-, c- and d- fractions correspond to the small-sized fraction ($R_t < R_{tM_p}$), at peak maximum ($R_t = R_{tM_p}$) and the large-sized fractions ($R_t > R_{tM_p}$ and $R_t \gg R_{tM_p}$), respectively. Fractions c and d are not available for AR04 and AR07.

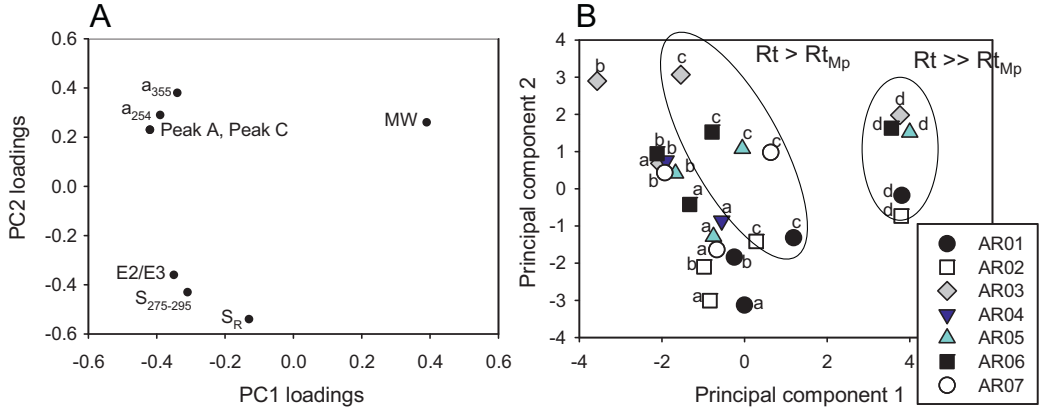

Fig. 9. Results of principal component analysis (PCA) of the optical properties and FlFFF based MW of AR samples. (A) Loading plots for PC1 and PC2. (B) Sample scores for the first two principal components (respectively, 59% and 36% of variance explained) of the PARAFAC score matrix. Letters are for (a) the small-sized fraction ($R_t < R_{tM_p}$), (b) at peak maximum ($R_t = R_{tM_p}$) and (c and d) the large-sized fractions ($R_t > R_{tM_p}$ and $R_t \gg R_{tM_p}$).

4. Conclusions

This study demonstrates that FlFFF-DAD-EEM system is effective for the analysis of DOM in bulk water without the need for isolation, fractionation and/or preconcentration. The linear range (5–30 ppm) and reproducibility (1.1% RSD) of the method explained herein has been shown to be suitable for aquatic DOM at environmentally relevant concentrations. Although higher concentrations (>10 ppm-C) could be injected, potential effects on separation, detection and integrity of the system should be carefully investigated. Another aspect to be considered is the inner filtering effect at high concentrations of absorbing molecules.

Based on the absorbance and fluorescence results shown herein, we conclude that DOM exhibits considerable variability in size distribution and spectral slope, as well as sizeable differences in absorption and fluorescence characteristics in general. Fluorescence peaked at a lower MW than absorbance, suggesting a different size distribution of fluorophores and chromophores in DOM. Further, the locations of humic-like peak maxima varied between samples, and between different size fractions of the same sample. These findings strongly suggest that freshwater DOM is not a uniform matrix of organic molecules, but rather consists of a range of constituents that have different molecular sizes and optical properties.

Acknowledgements

This work was funded National Sciences and Engineering Research Council of Canada and the Canada Research Chairs Program. CC gratefully acknowledges the financial support of the National Sciences and Engineering Research Council of Canada – Undergraduate Summer Research Program. We thank three anonymous reviewers for helpful comments and suggestions that helped improve the quality of this manuscript.

References

[1] N.V. Blough, R. Del Vecchio, in: D.A. Hansell, C.A. Carlson (Eds.), Biogeochemistry of Marine Dissolved Organic Matter, Academic Press, San Diego (2002) p. 509.
[2] C. Guéguen, L. Guo, N. Tanaka, Cont. Shelf Res. 25 (2005) 1195.
[3] C. Guéguen, L. Guo, D. Wang, N. Tanaka, C.C. Hung, Biogeochemistry 77 (2006) 139.
[4] N. Hudson, A. Baker, D. Reynolds, River Res. Appl. 23 (2007) 631.
[5] F.J. Stevenson, Humus Chemistry: Genesis, Composition, Reactions, Wiley and Sons, New York, 1994.
[6] C. Guéguen, J. Dominik, Appl. Geochem. 18 (2003) 457.
[7] C. Guéguen, B. Koukal, J. Dominik, M. Pardos, Chemosphere 53 (2003) 927.
[8] C. Guéguen, R. Gilbin, M. Pardos, J. Dominik, Appl. Geochem. 19 (2004) 153.
[9] R.G. Zepp, D.J. Erickson III, N.D. Paul, B. Sulzberger, Photochem. Photobiol. Sci. 6 (2007) 286.
[10] D.M. McKnight, G.R. Aiken, in: D.O. Hessen, L.J. Transvik (Eds.), Aquatic Humic Substances: Ecology and Biogeochemistry. Ecological Studies, Springer-Verlag, Berlin, 1998, p. 9.
[11] P.G. Coble, Chem. Rev. 107 (2007) 402.
[12] L. Guo, P.H. Santschi, in: K.J. Wilkinson, J.R. Lead (Eds.), Environmental Colloids and Particles: Behavior, Separation and Characterization, Wiley, Chichester, 2007, p. 159.
[13] C. Guéguen, C. Belin, J. Dominik, Water Res. 36 (2002) 1677.
[14] K. Mopper, Z. Feng, S.B. Bentjen, R.F. Chen, Mar. Chem. 55 (1996) 53.
[15] E. Zanardi-Lamardo, C.A. Moore, R.G. Yika, Mar. Chem. 89 (2004) 37.
[16] M. Hassellöv, Mar. Chem. 94 (2005) 111.
[17] S. Batchelli, F.L.L. Muller, M. Baalousha, J.R. Lead, Mar. Chem. 113 (2009) 227.
[18] J.C. Giddings, Sep. Sci. 1 (1966) 123.
[19] M. Hassellöv, F. von der Kammer, R. Beckett, in: K.J. Wilkinson, J.R. Lead (Eds.), Environmental Colloids and Particles: Behavior, Separation and Characterization, Wiley, Chichester, 2007, p. 159.
[20] R. Beckett, Z. Jue, J.C. Giddings, Environ. Sci. Technol. 21 (1987) 289.
[21] J.F. Ranville, M.J. Henry, T.N. Reszat, Q. Xie, B.D. Honeyman, J. Contam. Hydrol. 91 (2007) 233.
[22] S.A. Floge, M.L. Wells, Limnol. Oceanogr. 52 (2007) 32.
[23] F. von der Kammer, M. Baborowski, S. Tadjiki, W. Von Tümpling Jr., Acta Hydrochim. Hydrobiol. 31 (2003) 400.
[24] J. Moon, S.H. Kim, J. Cho, Colloids Surf. A: Physicochem. Eng. Aspects 287 (2006) 232.
[25] J. Boehme, M. Wells, Mar. Chem. 101 (2006) 95.
[26] C. Guéguen, M.A. Granskog, G. McCullough, D.G. Barber, J. Mar. Syst., 2010.
[27] J.R. Helms, A. Stubbins, J.D. Ritchie, E.C. Minor, Limnol. Oceanogr. 53 (2008) 955.
[28] W.W. Yau, J.J. Kirkland, D.D. Bly, Modern Size Exclusion Chromatography, Wiley, New York, 1979.
[29] J. Cho, G. Amy, J. Pellegrino, J. Mem. Sci. 164 (2000) 89.
[30] R. Beckett, M.E. Schimpf, in: M. Schimpf, K. Caldwell, J.C. Giddings (Eds.), Field-Flow Fractionation Handbook, Wiley-Interscience, New York, 2000, p. 497.
[31] B. Stolpe, L. Guo, A.M. Shiller, M. Hassellöv, Mar. Chem. 118 (2010) 119.
[32] I.T. Jolliffe, Principal Component Analysis 2e, Springer-Verlag Inc., New York, 2002.
[33] T. Persson, M. Wedborg, Anal. Chim. Acta 434 (2001) 179.
[34] J. Boehme, P. Coble, R. Conmy, A. Stovall-Leonard, Mar. Chem. 89 (2004) 3.
[35] C.A. Stedmon, S. Markager, Limnol. Oceanogr. 50 (2) (2005) 686.
[36] C.A. Stedmon, R. Bro, Limnol. Oceanogr.: Methods 6 (2008) 572.
[37] H. De Haan, T. De Boer, Water Res. 21 (1987) 731.
[38] L. Guo, P.H. Santschi, Mar. Chem. 55 (1996) 113.
[39] Q. Zhou, S.E. Cabaniss, P.A. Maurice, Water Res. 34 (2000) 3505.
[40] N. Her, G. Amy, D. Foss, J. Cho, Environ. Sci. Technol. 36 (2002) 3393.
[41] T.N. Reszat, M.J. Hendry, Anal. Chem. 77 (2005) 4195.
[42] I.A.M. Worms, Z. Al-Gorani Szigeti, S. Dubsacous, G. Lespes, J. Traber, L. Sigg, V.I. Slaveykova, Water Res. 44 (2010) 340.
[43] B. Lyven, M. Hassellöv, C. Haraldsson, D.R. Turner, Anal. Chim. Acta 397 (1997) 187.
[44] C. Minero, V. Lauri, G. Falletti, V. Maurino, E. Pelizzetti, D. Vione, Ann. Chim. 97 (2007) 1107.
[45] Y. Ran, L.M. Fu, G.Y. Sheng, R. Beckett, B.T. Hart, Chemosphere 41 (2000) 33.
[46] Y. Yang, D. Zhang, Commun. Soil Sci. Plant Anal. 26 (1995) 2333.
[47] M. Benedetti, J.F. Ranville, M. Ponthieu, J.P. Pinheiro, Org. Geochem. 33 (2002) 269.
[48] E. Bolea, M.P. Gorriz, M. Bouby, F. Laborda, J.R. Castillo, H. Geckeis, J. Chromatogr. A 1129 (2006) 236.
[49] J. Peuravouri, K. Pihlaja, Anal. Chim. Acta 337 (1997) 133.
[50] Y. Yamashita, N. Maie, H. Briceño, R. Jaffé, J. Geophys. Res. 115 (2010) G00F10, doi:10.1029/2009JG000987.
[51] P.G. Coble, Mar. Chem. 51 (1996) 325.
[52] C. Lønborg, X.A. Álvarez-Salgado, K. Davidson, S. Martínez-García, E. Teira, Mar. Chem. 119 (2010) 121.
[53] E. Parlanti, K. Wörz, L. Geoffroy, M. Lamotte, Org. Geochem. 31 (2000) 1765.
[54] Y. Yamashita, E. Tanoue, Mar. Chem. 82 (2003) 255.
[55] C. Belin, C. Quellec, M. Lamotte, M. Ewald, P. Simon, Environ. Technol. 14 (1993) 1131.
[56] F.C. Wu, R.D. Evans, P.J. Dillon, Environ. Sci. Technol. 37 (2003) 3687.
[57] N. Her, G. Amy, D. McKnight, J. Sohn, Y. Yoon, Water Res. 37 (2003) 4295.